Chapter 5

ENO and WENO Schemes

Y.-T. Zhang* and C.-W. Shu†
*University of Notre Dame, Notre Dame, IN, United States
†Brown University, Providence, RI, United States

Chapter Outline

ABSTRACT
The weighted essentially nonoscillatory (WENO) schemes, based on the successful essentially nonoscillatory (ENO) schemes with additional advantages, are a popular class of high-order accurate numerical methods for hyperbolic partial differential equations (PDEs) and other convection-dominated problems. The main advantage of such schemes is their capability to achieve arbitrarily high-order formal accuracy in smooth regions while maintaining stable, nonoscillatory and sharp discontinuity transitions. The schemes are thus especially suitable for problems containing both strong discontinuities and complex smooth solution structures. In this chapter, we review the basic formulation of ENO and WENO schemes, outline the main ideas in constructing the schemes and discuss several of recent developments in using the schemes to solve hyperbolic type PDE problems.

Keywords: Essentially nonoscillatory (ENO) schemes, Weighted essentially nonoscillatory (WENO) schemes, High-order accuracy, Hyperbolic partial differential equations, Convection-dominated problems, Finite volume schemes, Finite difference schemes

AMS Classification Code: 65M99

Handbook of Numerical Analysis, Vol. 17. http://dx.doi.org/10.1016/bs.hna.2016.09.009

1 INTRODUCTION

High-order accuracy numerical methods are especially efficient for solving partial differential equations (PDEs) which contain complex solution structures. Here we refer to high-order accurate numerical methods by those with an order of accuracy at least three, measured by local truncation errors when the solution is smooth. High-order numerical schemes have been applied extensively in computational fluid dynamics for solving convection-dominated problems with both discontinuities/sharp gradient regions and complicated smooth structures, for example, the Rayleigh–Taylor instability simulations (Remacle et al., 2003; Shi et al., 2003; Zhang et al., 2003, 2006b), the shock vortex interactions (Grasso and Pirozzoli, 2001; Zhang et al., 2005, 2006a, 2009) and direct simulation of compressible turbulence (Taylor et al., 2007). Its resolution power over the lower-order schemes was verified in these applications.

For hyperbolic PDEs or convection-dominated problems, their solutions can develop singularities such as discontinuities, sharp gradients, discontinuous derivatives, etc. For problems containing both singularities and complicated smooth solution structures, schemes with uniform high order of accuracy in smooth regions of the solution which can also resolve singularities in an accurate and essentially nonoscillatory (ENO) fashion are desirable, since a straightforward high-order approximation for the nonsmooth region of a solution will generate instability called Gibbs phenomena. A popular class of such schemes is the class of weighted essentially nonoscillatory (WENO) schemes. WENO schemes are designed based on the successful ENO schemes (Harten et al., 1987; Shu and Osher, 1988, 1989) with additional advantages. The first WENO scheme was constructed by Liu, Osher and Chan in their pioneering paper (Liu et al., 1994) for a third-order finite volume version. Jiang and Shu (1996) constructed arbitrary-order accurate finite difference WENO schemes for efficiently computing multidimensional problems, with a general framework for the design of the smoothness indicators and nonlinear weights. The fifth-order finite difference WENO scheme in Jiang and Shu (1996) has been used in most applications.

The main idea of the WENO schemes is to form a weighted combination of several local reconstructions based on different stencils (usually referred to as small stencils) and use it as the final WENO reconstruction. The combination coefficients (also called nonlinear weights) depend on the linear weights, often chosen to increase the order of accuracy over that on each small stencil, and on the smoothness indicators which measure the smoothness of the reconstructed function in the relevant small stencils. Hence an adaptive approximation or reconstruction procedure is actually the essential part of the WENO schemes.

In this article, we review the basic formulation of ENO and WENO schemes, describe the main ideas in constructing the finite volume and finite difference

versions of the schemes and emphasize several of recent developments in using the schemes to solve hyperbolic type PDE problems. The organization of this paper is as follows. ENO and WENO approximation or reconstruction procedure is explained in Section 2. In Section 3, we describe the finite volume and finite difference ENO/WENO schemes for solving hyperbolic conservation laws. Several recent developments are discussed in Section 4.

2 ENO AND WENO APPROXIMATIONS

The essential part of the ENO and WENO schemes is an adaptive approximation or reconstruction procedure. In this section, we describe the basic idea of this procedure using the third-order ENO and the fifth-order WENO approximations as examples.

2.1 Reconstruction

We first explain the reconstruction procedure which is the building block of all ENO and WENO approximations. For simplicity of the explanation, a uniform mesh $\cdots < x_0 < x_1 < x_2 < \cdots$ is used and the mesh size $\Delta x = x_{i+1} - x_i$ is a constant. The half-grid points $x_{i+1/2} = \frac{1}{2}(x_i + x_{i+1})$, and the domain is partitioned into computational cells $I_i = (x_{i-1/2}, x_{i+1/2})$, $i = \ldots, 0, 1, 2, \ldots$. We would like to emphasize that the uniform mesh assumption is not necessary for the reconstruction procedure here, although it may be needed for specific cases (for example, a uniform mesh or a smoothly varying mesh should be used in constructing a high-order conservative finite difference ENO or WENO scheme). Given the cell average values

$$\bar{u}_i = \frac{1}{\Delta x}\int_{x_{i-1/2}}^{x_{i+1/2}} u(x)dx \tag{1}$$

of a function $u(x)$ over the cells I_i for all i, we would like to find an approximation of $u(x)$ at a given point, for example, at the half-grid points $x_{i+1/2}$.

Lagrange interpolation technique can be applied here. Define the primitive function of $u(x)$ by

$$U(x) = \int_{x_{-1/2}}^{x} u(\xi)d\xi, \tag{2}$$

where the lower limit $x_{-1/2}$ is irrelevant and can be replaced by any other half-grid point, then the point values of the primitive function $U(x_{i+1/2})$ at all half-grid points can be obtained from the cell average values as the following

$$U(x_{i+1/2}) = \int_{x_{-1/2}}^{x_{i+1/2}} u(\xi)d\xi = \sum_{l=0}^{i} \Delta x \bar{u}_l. \tag{3}$$

Hence we can construct interpolation polynomials for $U(x)$, and approximate $u(x)$ by directly taking the derivative of the interpolation polynomials. Different stencils will lead to different approximations. For example, if we would like to find a polynomial $p_1(x)$ of degree at most two which reconstructs $u(x)$ on the stencil $S_1 = \{I_{i-2}, I_{i-1}, I_i\}$, namely,

$$(\bar{p}_1)_j = \frac{1}{\Delta x}\int_{x_{j-1/2}}^{x_{j+1/2}} p_1(x)dx = \bar{u}_j, \quad j = i-2, i-1, i, \tag{4}$$

a polynomial $P_1(x)$ of degree at most three will be constructed which interpolates the function $U(x)$ at the four half-grid points $x_{j+1/2}$, $j = i - 3, i - 2, i - 1, i$ and let $p_1(x) = P_1'(x)$. The condition (4) can be easily verified for such $p_1(x)$. Hence $u(x_{i+1/2})$ is approximated by $p_1(x_{i+1/2})$. Denoting the approximation by $u_{i+1/2}^{(1)} \triangleq p_1(x_{i+1/2})$, we have an explicit formula for it:

$$u_{i+1/2}^{(1)} = \frac{1}{3}\bar{u}_{i-2} - \frac{7}{6}\bar{u}_{i-1} + \frac{11}{6}\bar{u}_i. \tag{5}$$

This is a third-order accuracy approximation

$$u_{i+1/2}^{(1)} - u(x_{i+1/2}) = O(\Delta x^3), \tag{6}$$

if the function $u(x)$ is smooth in the stencil S_1. Similarly, if a different stencil $S_2 = \{I_{i-1}, I_i, I_{i+1}\}$ is chosen, we could find a different reconstruction polynomial $p_2(x)$ of degree at most two to satisfy $(\bar{p}_2)_j = \bar{u}_j$ for $j = i - 1, i, i + 1$. Then a different third-order accuracy approximation $u_{i+1/2}^{(2)} \triangleq p_2(x_{i+1/2})$ can be obtained if $u(x)$ is smooth in the stencil S_2. The formula is

$$u_{i+1/2}^{(2)} = -\frac{1}{6}\bar{u}_{i-1} + \frac{5}{6}\bar{u}_i + \frac{1}{3}\bar{u}_{i+1}. \tag{7}$$

The third choice of a approximation stencil to include the "target" cell I_i is $S_3 = \{I_i, I_{i+1}, I_{i+2}\}$. The third reconstruction polynomial $p_3(x)$ of degree at most two to satisfy $(\bar{p}_3)_j = \bar{u}_j$ for $j = i, i + 1, i + 2$ is constructed and gives another approximation $u_{i+1/2}^{(3)} \triangleq p_3(x_{i+1/2})$. Again the approximation has third-order accuracy if $u(x)$ is smooth in the stencil S_3. The explicit formula of this approximation is

$$u_{i+1/2}^{(3)} = \frac{1}{3}\bar{u}_i + \frac{5}{6}\bar{u}_{i+1} - \frac{1}{6}\bar{u}_{i+2}. \tag{8}$$

Remark 1. Another method of reconstruction is to directly find the polynomial whose averages on the stencil's cells agree with the given values by solving the resulting linear system. This method is convenient to be applied in reconstructions on unstructured meshes. Techniques such as using a closer to orthogonal basis and least square methods were developed to improve

the condition numbers of the linear system for reconstructions on high dimensional unstructured meshes. These two approaches result in the same reconstruction and hence the same error. For details, see Ciarlet and Raviart (1972), Abgrall et al. (1999), Abgrall and Sonar (1997) and Zhang and Shu (2003).

2.2 ENO Approximation

For hyperbolic PDEs or convection-dominated problems, solutions often have discontinuities (or sharp gradients). For such solutions, a fixed stencil approximation may not be adequate near discontinuities (or sharp gradient locations). Oscillations happen when the stencils contain the discontinuities (or sharp gradients).

The basic idea of ENO approximation is to adaptively avoid including the discontinuous cell (i.e., the cell on which the solution is discontinuous) in the stencil, if possible (Harten et al., 1987; Shu and Osher, 1988). For the reconstructions in Section 2.1, the ENO approximation is to choose one of the three approximations $u^{(1)}_{i+1/2}$, $u^{(2)}_{i+1/2}$ and $u^{(3)}_{i+1/2}$ given by (5), (7) and (8), respectively, based on the three stencils S_1, S_2 and S_3. The selection criterion is to compare the local smoothness of the reconstruction polynomials, measured by divided differences. Here we describe the procedure to construct a third-order ENO approximation. The job is to find a stencil which must include $x_{i-1/2}$ and $x_{i+1/2}$, such that the primitive function $U(x)$ (hence the corresponding reconstruction polynomial) is the "smoothest" in this stencil comparing with other possible stencils. The divided differences of $U(x)$ are used. We emphasize here that in the implementation of the procedure, the divided differences of $U(x)$ can be expressed completely by the divided differences of the given cell averages $\bar{u}$, without any need to reference $U(x)$ (Harten et al., 1987; Shu and Osher, 1988, 1989). Thus in cell I_i we start with a two point stencil $\widetilde{S}_2(i) = \{x_{i-1/2}, x_{i+1/2}\}$ for $U(x)$, which is equivalent to a one cell stencil $\bar{S}_1(i) = \{I_i\}$ for $\bar{v}$. Next we have two choices to expand the stencil by adding either the left neighbour $x_{i-3/2}$ or the right neighbour $x_{i+3/2}$. This is decided by comparing the absolute values of two relevant divided differences $U[x_{i-3/2}, x_{i-1/2}, x_{i+1/2}]$ and $U[x_{i-1/2}, x_{i+1/2}, x_{i+3/2}]$, and a smaller one implies that the function is "smoother" in that stencil. So, if

$$|U[x_{i-3/2}, x_{i-1/2}, x_{i+1/2}]| < |U[x_{i-1/2}, x_{i+1/2}, x_{i+3/2}]|, \tag{9}$$

the three-point stencil will be taken as

$$\widetilde{S}_3(i) = \{x_{i-3/2}, x_{i-1/2}, x_{i+1/2}\}; \tag{10}$$

otherwise, we will take the stencil

$$\widetilde{S}_3(i) = \{x_{i-1/2}, x_{i+1/2}, x_{i+3/2}\}. \tag{11}$$

This procedure can be repeated to add the next grid point to the stencil, according to the smaller of the absolute values of two relevant divided differences. For a third-order approximation, with one more grid point we will obtain the desired stencil, and one of the approximations $u^{(1)}_{i+1/2}, u^{(2)}_{i+1/2}$ or $u^{(3)}_{i+1/2}$ will be the final ENO approximation. Of course we can continue this procedure to add more grid points to the stencil for a higher-order accuracy ENO approximation.

2.3 WENO Approximation

WENO approximation is based on ENO, with additional advantages. For example, WENO approximation has higher-order accuracy than ENO approximation on the same stencils used in forming the reconstructions. WENO approximation results in more smooth numerical flux than ENO one when it is applied in solving a hyperbolic PDE.

The basic idea of WENO approximation is the following: instead of using only one of the candidate stencils to form the reconstruction, one uses a convex combination of all of them. If all three stencils S_1, S_2 and S_3 of a third-order ENO approximation are combined to form a large stencil $S = \{I_{i-2}, I_{i-1}, I_i, I_{i+1}, I_{i+2}\}$, a reconstruction polynomial $p(x)$ of degree at most four is obtained. $p(x)$ satisfies $\bar{p}_j = \bar{u}_j$, for $j = i-2, i-1, i, i+1, i+2$ and gives an approximation $u_{i+1/2} \triangleq p(x_{i+1/2})$. The explicit formula is

$$u_{i+1/2} = \frac{1}{30}\bar{u}_{i-2} - \frac{13}{60}\bar{u}_{i-1} + \frac{47}{60}\bar{u}_i + \frac{9}{20}\bar{u}_{i+1} - \frac{1}{20}\bar{u}_{i+2}. \tag{12}$$

Notice that this is a fifth-order accurate approximation if the function $u(x)$ is smooth in the large stencil S. Further investigation on the fifth-order approximation $u_{i+1/2}$ in (12) and the three third-order approximations $u^{(1)}_{i+1/2}, u^{(2)}_{i+1/2}$ and $u^{(3)}_{i+1/2}$, defined by (5), (7) and (8) reveals the following linear combination relationship:

$$u_{i+1/2} = \gamma_1 u^{(1)}_{i+1/2} + \gamma_2 u^{(2)}_{i+1/2} + \gamma_3 u^{(3)}_{i+1/2}, \tag{13}$$

where the constants γ_1, γ_2 and γ_3, satisfying $\gamma_1 + \gamma_2 + \gamma_3 = 1$, are called the linear weights. In this case they take values

$$\gamma_1 = \frac{1}{10}, \quad \gamma_2 = \frac{3}{5}, \quad \gamma_3 = \frac{3}{10}. \tag{14}$$

To deal with the situation that $u(x)$ is not smooth, WENO approximation uses the "nonlinear weights" technique to adaptively avoid including the discontinuous cell in the stencil. It chooses the final approximation as a convex combination of the three third-order approximations $u^{(1)}_{i+1/2}, u^{(2)}_{i+1/2}$ and $u^{(3)}_{i+1/2}$:

$$u_{i+1/2} = w_1 u^{(1)}_{i+1/2} + w_2 u^{(2)}_{i+1/2} + w_3 u^{(3)}_{i+1/2}, \tag{15}$$

where $w_j \geq 0$, and $w_1 + w_2 + w_3 = 1$. The nonlinear weight w_j is determined by the "smoothness indicator" β_j, which measures the relative smoothness of the function $u(x)$ in the stencil S_j. A larger β_j indicates that the function $u(x)$ is less smooth in the stencil S_j. In most of the WENO papers, the smoothness indicator β_j is chosen as in Jiang and Shu (1996),

$$\beta_j = \sum_{l=1}^{k} \Delta x^{2l-1} \int_{x_{i-1/2}}^{x_{i+1/2}} \left(\frac{d^l}{dx^l} p_j(x) \right)^2 dx, \tag{16}$$

where k is the polynomial degree of $p_j(x)$ (here, $k = 2$). This is a scaled sum of the square L^2 norms of all the derivatives of the relevant reconstruction polynomial $p_j(x)$ in the relevant cell I_i, with the scaling factor Δx^{2l-1} to make the final explicit formulas for the smoothness indicators independent on the grid size Δx. In this example, the explicit formulas of the smoothness indicators are the following quadratic functions of the cell average values of $u(x)$ in the relevant stencils:

$$\begin{aligned}
\beta_1 &= \frac{13}{12}(\bar{u}_{i-2} - 2\bar{u}_{i-1} + \bar{u}_i)^2 + \frac{1}{4}(\bar{u}_{i-2} - 4\bar{u}_{i-1} + 3\bar{u}_i)^2, \\
\beta_2 &= \frac{13}{12}(\bar{u}_{i-1} - 2\bar{u}_i + \bar{u}_{i+1})^2 + \frac{1}{4}(\bar{u}_{i-1} - \bar{u}_{i+1})^2, \\
\beta_3 &= \frac{13}{12}(\bar{u}_i - 2\bar{u}_{i+1} + \bar{u}_{i+2})^2 + \frac{1}{4}(3\bar{u}_i - 4\bar{u}_{i+1} + \bar{u}_{i+2})^2.
\end{aligned} \tag{17}$$

With these smoothness indicators, the nonlinear weights are defined as

$$w_j = \frac{\alpha_j}{\alpha_1 + \alpha_2 + \alpha_3}, \quad \alpha_j = \frac{\gamma_j}{(\epsilon + \beta_j)^2}, \quad j = 1, 2, 3. \tag{18}$$

Here ϵ is a small positive number used to avoid the denominator becoming zero and is typically chosen to be $\epsilon = 10^{-6}$ in computations. It is verified in Jiang and Shu (1996) that with such nonlinear weights, the WENO approximations (15) is fifth-order accurate if the function $u(x)$ is smooth in the large stencil S. If $u(x)$ is not smooth in a stencil S_j but is smooth in at least one of the other two stencils, the WENO approximations would guarantee a nonoscillatory result since the contribution from any stencil containing the discontinuity of $u(x)$ has an essentially zero weight.

Remark 2. There may be situations in which all small stencils contain the discontinuity. For example, there may be a discontinuity point in the cell I_i. It turns out that this seemingly difficult case is actually not problematic in ENO or WENO approximations, because the reconstruction polynomials are all essentially monotone in I_i (Harten et al., 1986).

3 ENO AND WENO SCHEMES FOR HYPERBOLIC CONSERVATION LAWS

In this section, we describe the finite volume and finite difference ENO and WENO schemes for solving hyperbolic conservation laws. First the simple one-dimensional scalar equation

$$u_t + f(u)_x = 0 \tag{19}$$

is used to show the ideas of constructing the schemes.

3.1 Finite Volume Schemes

In finite volume schemes, the integral form of the conservation law (19)

$$\frac{d\bar{u}_i(t)}{dt} + \frac{1}{\Delta x_i}\left(f(u_{i+1/2}) - f(u_{i-1/2})\right) = 0 \tag{20}$$

is considered. Here $\bar{u}_i = \dfrac{1}{\Delta x_i}\displaystyle\int_{I_i} u(x,t)dx$ is the spatial cell average of the solution $u(x, t)$ in the cell I_i. For linear stability of the schemes, upwinding property (i.e. numerical schemes should propagate solution information in the same characteristic direction as that of a hyperbolic PDE) is required. We replace $f(u_{i+1/2})$ by $\hat{f}(u^-_{i+1/2}, u^+_{i+1/2})$, where $\hat{f}(a,b)$ is a monotone numerical flux satisfying the following conditions: (1) $\hat{f}(a,b)$ is nondecreasing in its first argument and nonincreasing in its second argument; (2) $\hat{f}(a,b)$ is consistent with the physical flux $f(u)$, i.e., $\hat{f}(u,u) = f(u)$; (3) $\hat{f}(a,b)$ is Lipschitz continuous with respect to both arguments. Some examples of monotone fluxes include the Godunov flux

$$\hat{f}(a,b) = \begin{cases} \min_{a\le x\le b} f(u) & \text{if } a \le b, \\ \max_{b\le x\le a} f(u) & \text{if } a > b; \end{cases} \tag{21}$$

the Engquist–Osher flux

$$\hat{f}(a,b) = \int_0^a \max(f'(u),0)du + \int_0^b \min(f'(u),0)du + f(0); \tag{22}$$

and the Lax–Friedrichs flux

$$\hat{f}(a,b) = \frac{1}{2}[f(a) + f(b) - \alpha(b-a)], \tag{23}$$

where $\alpha = \max_u |f'(u)|$ is a constant and the maximum is taken over the relevant range of u. $u^-_{i+1/2}$ and $u^+_{i+1/2}$ are ENO/WENO approximations based on cell average values in stencils one cell biased to the left and one cell biased to the right, respectively. For a third-order ENO or a fifth-order WENO scheme, the

approximation $u^-_{i+1/2}$ uses cell average values in cells $\{I_{i-2}, I_{i-1}, I_i, I_{i+1}, I_{i+2}\}$, while the approximation $u^+_{i+1/2}$ uses those in cells $\{I_{i-1}, I_i, I_{i+1}, I_{i+2}, I_{i+3}\}$. Section 2 gives the detailed procedure for these ENO/WENO reconstructions.

With a monotone numerical flux and ENO/WENO reconstructions, the integral form (20) can be written as a method-of-lines ordinary differential equation (ODE) system

$$\frac{d\bar{u}_i(t)}{dt} = -\frac{1}{\Delta x_i}\left[\hat{f}(u^-_{i+1/2}, u^+_{i+1/2}) - \hat{f}(u^-_{i-1/2}, u^+_{i-1/2})\right]. \tag{24}$$

The ODE system can be discretized by a high-order total variation diminishing (TVD) Runge–Kutta time discretization method, also known as the strong stability preserving (SSP) method (Gottlieb et al., 2001; Shu and Osher, 1988). For example, the most popular TVD Runge–Kutta method is the third-order accurate one given in Shu and Osher (1988). Other time discretization methods may also be applied. For example, the method which uses a Lax–Wendroff procedure to convert all time derivatives into spatial derivatives and discretizes all the spatial derivatives to the correct order of accuracy, e.g., see Harten et al. (1987), Titarev and Toro (2005) and Qiu and Shu (2003).

3.2 Finite Difference Schemes

Finite difference schemes use point values $\{u_i\}$ of the numerical solution to approximate the PDE directly. A finite difference scheme for hyperbolic conservation laws is required to be in conservation form. For Eq. (19), it is

$$\frac{du_i(t)}{dt} + \frac{1}{\Delta x}\left(\hat{f}_{i+1/2} - \hat{f}_{i-1/2}\right) = 0, \tag{25}$$

where $\hat{f}$ is the numerical flux. $\hat{f}_{i+1/2} = \hat{f}(u_{i-p}, \ldots, u_{i+q})$, and it is consistent with the physical flux $\hat{f}(u, \ldots, u) = f(u)$ and is Lipschitz continuous with respect to all its arguments. The scheme is r-th order accurate if

$$\frac{1}{\Delta x}\left(\hat{f}_{i+1/2} - \hat{f}_{i-1/2}\right) = f(u)_x|_{x=x_i} + O(\Delta x^r), \tag{26}$$

when $u(x)$ is smooth in the stencil.

It was found in Shu and Osher (1989) that one can directly use the same ENO/WENO reconstruction procedure in a finite volume scheme to compute the numerical flux $\hat{f}_{i+1/2}$. By defining the cell averages $\bar{h}_i$ of a function $h(x)$ to be $\bar{h}_i \triangleq f(u_i)$, we apply the high-order accuracy ENO/WENO approximation in Section 2 to compute the point values $h(x_{i+1/2})$. Then the numerical flux is obtained

$$\hat{f}_{i+1/2} = h(x_{i+1/2}). \tag{27}$$

For the purpose of linear stability (upwinding), a flux splitting is performed, i.e.

$$f(u) = f^+(u) + f^-(u), \tag{28}$$

where $f^+(u)$ and $f^-(u)$ satisfy $\frac{d}{du}f^+(u) \geq 0, \frac{d}{du}f^-(u) \leq 0$. Upwinding requires that the approximation $\hat{f}^+_{i+1/2}$ for $f^+(u_{i+1/2})$ uses a biased stencil with one more point to the left, and $\hat{f}^-_{i+1/2}$ for $f^-(u_{i+1/2})$ uses a biased stencil with one more point to the right. A very popular flux splitting is the Lax–Friedrichs splitting

$$f^+(u) = \frac{1}{2}(f(u) + \alpha u), \quad f^-(u) = \frac{1}{2}(f(u) - \alpha u), \tag{29}$$

where $\alpha = \max_u |f'(u)|$. Other flux splittings can also be used (Jiang and Shu, 1996). Using the high-order accuracy ENO/WENO approximation to obtain $\hat{f}^+_{i+1/2}$ and $\hat{f}^-_{i+1/2}$, we have the final numerical flux

$$\hat{f}_{i+1/2} = \hat{f}^+_{i+1/2} + \hat{f}^-_{i+1/2}. \tag{30}$$

The resulting ODE system (25) can again be evolved by a high-order time discretization scheme, for example, the third-order accurate TVD Runge–Kutta method.

3.3 Remarks on Multidimensional Problems and Systems

In this section, we make several remarks about using ENO/WENO schemes in solving multidimensional problems and PDE systems. A high-order finite difference scheme for solving a multidimensional problem can be performed dimension by dimension directly on a uniform Cartesian or a smooth curvilinear mesh. Its computational cost is exactly the same as in the one-dimensional case per point per direction. However, for nonuniform and unstructured meshes, high-order finite difference scheme can *not* be applied and a finite volume scheme has to be used. A high-order finite volume scheme is generally more expensive than a finite difference scheme of the same order of accuracy if the same mesh and the same reconstruction procedure are used, since even on a Cartesian mesh, the direct dimension by dimension ENO/WENO reconstruction can *not* be performed for a nonlinear hyperbolic conservation law. For example, in two dimensions, a finite volume scheme with accuracy order higher than two is two to five times as expensive as a finite difference one, depending on the specific coding and computer type. This discrepancy in cost is even bigger for higher dimension problems. A detailed comparison of finite volume and finite difference schemes for solving multidimensional problems in the context of ENO approximations can be found in Casper et al. (1994).

For systems of hyperbolic conservation laws, the ENO/WENO schemes have the same structure as those for the scalar cases. A monotone flux is replaced by an exact or approximate Riemann solver (Toro, 2009). The ENO/WENO reconstruction can be performed either componentwise or in local characteristic directions. Usually, componentwise reconstruction produces satisfactory results for schemes up to third-order accuracy, while characteristic reconstruction produces better nonoscillatory results for higher-order accuracy, albeit with an increased computational cost. Details about the local characteristic decomposition procedure can be found in, e.g., Harten et al. (1987), Shu and Osher (1988) and Shu et al. (1992).

4 SELECTED TOPICS OF RECENT DEVELOPMENTS

In this section, we discuss a few selected topics of recent developments in using ENO/WENO schemes to solve hyperbolic or convection–diffusion problems.

4.1 Unstructured Meshes

While ENO/WENO schemes on structured (either Cartesian or smooth curvilinear) meshes are quite mature, the development of simple and robust ENO/WENO schemes on unstructured meshes (e.g. arbitrary triangular or tetrahedral meshes) for dealing with complex domain geometries is less advanced. The finite volume approach must be used to design ENO/WENO schemes on unstructured meshes for solving hyperbolic conservation laws. We use the two-dimensional conservation law

$$\frac{\partial u}{\partial t}+\frac{\partial f(u)}{\partial x}+\frac{\partial g(u)}{\partial y}=0 \tag{31}$$

as an example, and the computational control volumes are triangles $\{\triangle_i\}$. The semidiscrete finite volume scheme of (31) is formulated as

$$\frac{d\bar{u}_i(t)}{dt}+\frac{1}{|\triangle_i|}\int_{\partial\triangle_i} F\cdot n dS=0 \tag{32}$$

where the cell average $\bar{u}_i(t)=\dfrac{1}{|\triangle_i|}\displaystyle\int_{\triangle_i} u dxdy$, $F=(f,g)^T$, and n is the outward unit normal of the triangle boundary $\partial\triangle_i$. In (32), the line integral is discretized by a q-point Gaussian quadrature formula,

$$\int_{\partial\triangle_i} F\cdot n ds\approx\sum_{k=1}^{3}S_k\sum_{j=1}^{q}\tilde{w}_j F\left(u\left(G_j^{(k)},t\right)\right)\cdot n_k \tag{33}$$

where S_k is the length of the k-th side of $\partial\triangle_i$, $G_j^{(k)}$ and $\tilde{w}_j$ are the Gaussian quadrature points and weights, respectively, and $F\left(u\left(G_j^{(k)},t\right)\right)\cdot n_k$ is

approximated by a numerical flux. For example, if the Lax–Friedrichs flux is used, then we have

$$F\left(u\left(G_j^{(k)},t\right)\right)\cdot n_k \approx \frac{1}{2}\left[\left(F\left(u^-\left(G_j^{(k)},t\right)\right)+F\left(u^+\left(G_j^{(k)},t\right)\right)\right)\cdot n_k-\alpha\left(u^+\left(G_j^{(k)},t\right)-u^-\left(G_j^{(k)},t\right)\right)\right], \tag{34}$$

where α is taken as an upper bound for the magnitude of the eigenvalues of the Jacobian in the n_k direction, and u^- and u^+ are the values of u inside the triangle and outside the triangle (inside the neighbouring triangle) at the Gaussian point. q is determined by the order of accuracy of the schemes. For example, if a third-order finite volume scheme is designed, then the two-point Gaussian quadrature $q = 2$ is used. For the line with endpoints P_1 and P_2, the Gaussian quadrature points are $G_1 = cP_1 + (1 - c)P_2$, $G_2 = cP_2 + (1 - c)P_1$, where $c=\frac{1}{2}+\frac{\sqrt{3}}{6}$; and the Gaussian quadrature weights are $\tilde{w}_1=\tilde{w}_2=\frac{1}{2}$.

The next key step is to build a high-order ENO/WENO reconstruction for the point values at the Gaussian quadrature points. About the development of high-order ENO reconstructions on unstructured meshes, the reader is referred to Abgrall (1994), Abgrall and Sonar (1997) and Augoula and Abgrall (2000). For WENO reconstructions, the big stencil S consisting of triangles is a union of small stencils $\{S_m : m = 1, 2, \ldots, N\}$. Cell average values of u in S are used to construct a polynomial $p(x, y)$, which will have the same cell average as u on the target cell $\triangle_0$ (i.e., the control volume cell). WENO reconstructions need to obtain a linear combination of reconstructions on small stencils. The reconstruction values at the Gaussian points should satisfy

$$p\left(x^G,y^G\right)=\sum_{m=1}^{N}\gamma_m p_m\left(x^G,y^G\right), \tag{35}$$

where (x^G, y^G) is a Gaussian point, p_m is a reconstruction polynomial on a small stencil S_m, and γ_m is the linear weight. Based on (35), nonlinear WENO reconstruction values at the Gaussian points are

$$p_{\text{weno}}\left(x^G,y^G\right)=\sum_{m=1}^{N}\omega_m p_m\left(x^G,y^G\right), \tag{36}$$

where ω_m is a nonlinear WENO weight defined as

$$\omega_m=\frac{\tilde{\omega}_m}{\sum_{m=1}^{N}\tilde{\omega}_m},\qquad \tilde{\omega}_m=\frac{\gamma_m}{(\epsilon+IS_m)^2}. \tag{37}$$

As that for the WENO reconstructions on structured meshes, IS_m is the smoothness indicator for the m-th reconstruction polynomial $p_m(x, y)$ associated with the m-th small stencil S_m, and ϵ is a small positive number to avoid the denominator to become 0. The smoothness indicator measures how smooth the function p_m is on the target cell $\triangle_0$: the smaller the smoothness indicator, the smoother the function p_m is on $\triangle_0$. For two-dimensional problems, it is defined as

$$IS_m = \sum_{1 \le |\alpha| \le k} \int_{\triangle_0} |\triangle_0|^{|\alpha|-1} (D^\alpha p_m(x,y))^2 dxdy, \tag{38}$$

where k is the degree of polynomial p_m, α is a multiindex and D is the derivative operator. For the definition of the smoothness indicator for three-dimensional problems, the reader is referred to Zhang and Shu (2009).

There are two types of WENO reconstructions on unstructured meshes in the literature. The major difference between them is the different method to construct small stencils and find linear weights. The first type (type I) reconstruction has an order of accuracy not higher than that of the reconstruction on each small stencil. This is similar as ENO schemes. For this type of WENO reconstructions, the nonlinear weights do not contribute towards the increase of the order of accuracy, and they are designed purely for the purpose of nonlinear stability, or to avoid spurious oscillations. Because type I WENO schemes just need to choose the linear weights as arbitrary positive numbers for better linear stability (e.g. the centred small stencil is assigned a larger linear weight than the others), they are easier to construct than the type II WENO schemes discussed in the following paragraph. For Type I WENO reconstructions, see e.g., Friedrichs (1998) and Titarev et al. (2010) for two-dimensional triangulations and Dumbser and Käser (2007) and Dumbser et al. (2007) for three-dimensional triangulations.

The second type (type II) consists of WENO schemes whose order of accuracy is higher than that of the reconstruction on each small stencil. For example, the third-order WENO scheme on two-dimensional triangular meshes in Hu and Shu (1999) is based on second-order accuracy linear polynomial reconstructions on small stencils, and the fourth-order WENO scheme in Hu and Shu (1999) is based on third-order accuracy quadratic polynomial reconstructions on small stencils. For similar WENO schemes on two-dimensional triangular meshes for solving Hamilton–Jacobi equations, we refer to see Zhang and Shu (2003) and Levy et al. (2006) and for WENO reconstructions on three-dimensional tetrahedral meshes, which belong to type II as well, we refer to see Zhang and Shu (2009). Type II WENO schemes are more difficult to construct, however they have a much more compact stencil than type I WENO schemes of the same accuracy, which is an advantage in applications, such as when the WENO methodology is used as limiters for the discontinuous Galerkin methods, e.g., Qiu and Shu (2005)

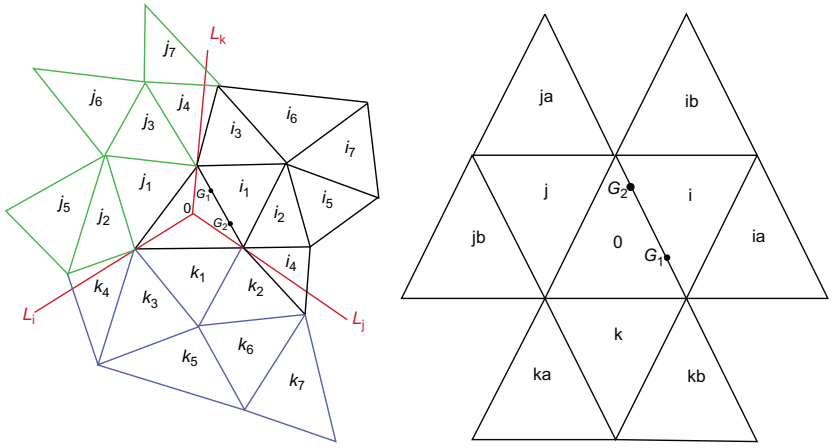

FIG. 1 A big stencil S for a third-order WENO reconstruction. *Left*: the type I; *right*: the type II. *Pictures are reproduced from Liu, Y., Zhang, Y.T., 2013. A robust reconstruction for unstructured WENO schemes. J. Sci. Comput. 54, 603–621, with permission of Springer.*

and Zhu et al. (2008). For example, see the big stencil S for a third-order WENO reconstruction of type I and II in Fig. 1. The type I reconstruction needs more layers of neighbouring triangles of the target cell $\triangle_0$ (i.e., the cell "0" in Fig. 1) than that for the type II reconstruction. Actually the big stencil of the type II reconstruction (the right picture in Fig. 1) is just the central small stencil in the type I reconstruction.

A crucial step in building a type II WENO scheme on unstructured meshes is to construct lower-order polynomials whose weighted average will give the same result as the high-order reconstruction at each Gaussian quadrature point for the flux integral on the element boundary. This step is actually the most difficult step in designing a robust second type high-order WENO schemes on unstructured meshes, since we can not guarantee the quality of the unstructured meshes when the domain geometry is very complicated. Especially, when the spatial domain has higher dimensions (e.g. three-dimensional problems) and complex geometry, the quality of the unstructured meshes is hard to control. Distorted local mesh geometries can be easily generated. The local linear system for finding linear weights could have very large condition number or is even singular at the places where mesh quality is bad (e.g. there are very obtuse triangles). This may lead to negative and very large linear weights in type II WENO schemes, or even the linear weights do *not* exist. For mild negative linear weights, the splitting technique developed in Shi et al. (2002) can be applied effectively. For the degenerate cases in various mesh geometries that linear weights are negative and very large or do *not* exist, a more robust approach is needed. In a recent work (Liu and Zhang, 2013), we hybrid the approaches of type II and type I WENO schemes, and avoid

the appearance of negative and very large linear weights no matter how bad the quality of the unstructured meshes is. The idea is to switch to the approach of assigning linear weights of type I WENO schemes at the places where the linear weight system of type II WENO scheme is ill-posed or singular, i.e., the linear weights are negative and very large (larger than a preset threshold value) or do *not* exist. The trade-off is that the compactness of the type II WENO scheme will be lost at these places. But we obtain a robust reconstruction with respect to the quality of unstructured meshes and the complexity of the domain. Furthermore, since for a general triangulation distorted mesh geometries only occur in minor parts of the whole domain, the overall percentage of the places where the type I WENO approach is applied is quite small. We refer to Liu and Zhang (2013) for more details.

4.2 Steady State Problems

Steady state problems for hyperbolic PDEs are common mathematical models appearing in many applications, such as fluid mechanics, optimal control, differential games, image processing and computer vision, geometric optics, etc. Solution information of these boundary value problems propagates along characteristics starting from the boundary. A large nonlinear system is obtained after spatial discretization of a steady state hyperbolic PDE by a high-order WENO scheme. It is still a challenging problem how to solve the large nonlinear system resulting from WENO discretization.

There are at least two factors which may affect efficiency and robustness of computation. One is that a high-order accurate shock capturing scheme such as a WENO scheme often suffers from difficulties in its convergence towards steady state solutions. In Zhang and Shu (2007), a systematic study was carried out and discovered that slight postshock oscillations actually cause this problem. A new smoothness indicator (Zhang and Shu, 2007) and upwind-biased interpolation technique (Zhang et al., 2011) have been developed to improve the convergence of fifth-order WENO scheme for solving steady state of Euler systems. The other factor affecting the performance of computation is the iterative scheme designed for the nonlinear system.

For a highly nonlinear system derived from high-order WENO spatial discretization, one way is to solve it directly with Newton iterations (e.g. Hu et al., 2011), or a more robust method such as the homotopy method (Hao et al., 2013). A major advantage of solving the nonlinear system by Newton iterations or the homotopy method is that the resulting methods are free of the CFL condition, hence have linear computational complexity in solving these boundary value problems. Another way is to solve the large WENO system by fixed-point iterative schemes of Jacobi type or Gauss–Seidel type. The popular time marching approach for solving steady state problems is essentially a Jacobi type fixed-point iterative method. Starting from an initial condition, the numerical solution evolves into a steady state by using a time

stepping scheme (e.g. Abgrall and Mezine, 2004; Abgrall and Roe, 2003; Chou and Shu, 2006; Jiang and Shu, 1996). A big advantage of the time marching method is that the computed steady state is stable and usually carries physical properties of the system and the initial condition. However, the computational efficiency of time marching method for obtaining a steady state solution is restricted by the CFL condition. This can be improved by the "fast sweeping" technique. Fast sweeping methods utilize alternating sweeping strategy to cover a family of characteristics in a certain direction simultaneously in each sweeping order. Coupled with the Gauss–Seidel iterations, these methods can achieve a fast convergence speed for computations of steady state solutions of hyperbolic PDEs by high-order WENO schemes (Xiong et al., 2010; Zhang et al., 2006c,d).

Furthermore, to compute steady state of hyperbolic conservation laws, the forward Euler time marching is preferred since only one stage and one step is used, as time direction accuracy has no effects on the numerical accuracy of steady state solutions. However, a high-order WENO scheme (e.g. the fifth-order WENO scheme) coupled with the first-order forward Euler time discretization is linearly unstable (Wang and Spiteri, 2007). Hence a high-order time discretization needs to be coupled with a high-order WENO scheme for steady state problems, which increases the number of iterations for the Jacobi type fixed-point scheme to converge. In a recent work (Wu et al., 2016), based on fifth-order WENO schemes which improve the convergence of the classical WENO schemes by removing slight postshock oscillations (Zhang and Shu, 2007; Zhang et al., 2011), we designed fifth-order fixed-point sweeping WENO methods for steady state of hyperbolic conservation laws. It is discovered that the fast sweeping technique can largely improve the stability of high-order spatial scheme with the forward Euler time marching. Extensive numerical experiments are performed in Wu et al. (2016) to compare four different iterative schemes including the regular forward Euler and Runge–Kutta time marching methods, and the ones coupled with fast sweeping technique. All numerical examples show that the forward Euler time discretization with fast sweeping technique is the most efficient approach for fifth-order WENO computations of steady state of hyperbolic conservation laws.

4.3 Time Discretizations for Convection–Diffusion Problems

High-order WENO schemes are often used to discretize nonlinear convection terms for convection–diffusion PDEs, to deal with the convection-dominated cases or a spatial mixture of convection-dominated and diffusion-dominated cases. A general convection–diffusion problem may contain significant diffusion in some regions and couple nonlinear stiff reaction terms, with dominated convection in other regions. Computational efficiency by using high-order WENO schemes to solve such problems depends heavily on robust time discretizations which permit large time step sizes, since the regular explicit time

schemes require very small time step sizes. A fully implicit discretization by using implicit Runge–Kutta or backward difference formula (BDF) methods (see, e.g. Hairer and Wanner, 1991) has large linear stability regions but typically requires the solution of large nonlinear coupled system of algebraic equations. Especially high-order WENO schemes have high level of nonlinearity in the nonlinear weights. Certain iterative schemes such as Newton's method do not seem to be robust near strong shocks for a large time step, and special treatment is required (Gottlieb et al., 2006). Another approach is to avoid solving completely coupled nonlinear systems, for example, to use implicit–explicit (IMEX) Runge–Kutta methods (see, e.g. Kennedy and Carpenter, 2003). To deal with stiffness in a convection–diffusion–reaction problem, exponential integrator is an efficient tool. Recently, implicit integration factor (IIF) WENO methods were developed for solving stiff nonlinear convection–diffusion–reaction equations (Jiang and Zhang, 2013). The methods can be designed for arbitrary order of accuracy and no large nonlinear coupled algebraic system needs to be solved. The stiffness of the system is resolved well and the methods are stable by using time step sizes which are mainly determined by the nonstiff hyperbolic part of the system. To efficiently calculate large matrix exponentials, Krylov subspace approximation is applied in the methods. The time discretizations in Jiang and Zhang (2013) are multistep methods. In Jiang and Zhang (2016), single-step IIF-WENO methods were developed for solving stiff convection–diffusion–reaction equations. The methods are designed carefully to avoid generating positive exponentials in the matrix exponentials, which is necessary for the stability of the exponential integrator schemes.

4.4 Accuracy Enhancement

Efforts have been made to improve the accuracy in high-order WENO schemes. Strategies include modifying the linear or nonlinear weights, modifying the smoothness indicators, or improving the dissipation and/or dispersion properties of WENO schemes. For example, in Henrick et al. (2005), a mapping function was designed to modify the nonlinear weights in Jiang and Shu (1996). The resulting nonlinear weights improve accuracy of the WENO schemes at smooth extrema. In Borges et al. (2008) and Castro et al. (2011), the classical smoothness indicators in Jiang and Shu (1996) were combined to form new smoothness indicators, which also improve accuracy and resolution of the WENO schemes without the mapping. For high frequency wave computations, the resolution can be enhanced via optimizing the dissipation and/or dispersion of the WENO schemes (for example, see Hu et al., 2015; Martin et al., 2006; Ponziani et al., 2003; Wang and Chen, 2001).

ACKNOWLEDGEMENTS

This research was supported by NSF grants DMS-1620108 and DMS-1418750.

REFERENCES

Abgrall, R., 1994. On essentially non-oscillatory schemes on unstructured meshes: analysis and implementation. J. Comput. Phys. 114, 45–58.

Abgrall, R., Mezine, M., 2004. Construction of second order accurate monotone and stable residual distribution schemes for steady problems. J. Comput. Phys. 195, 474–507.

Abgrall, R., Roe, P.L., 2003. High order fluctuation scheme on triangular meshes. J. Sci. Comput. 19, 3–36.

Abgrall, R., Sonar, T., 1997. On the use of Muehlbach expansions in the recovery step of ENO methods. Numer. Math. 76, 1–25.

Abgrall, R., Lantéri, S., Sonar, T., 1999. ENO approximations for compressible fluid dynamics. ZAMM - J. Appl. Math. Mech. 79, 3–28.

Augoula, S., Abgrall, R., 2000. High order numerical discretization for Hamilton-Jacobi equations on triangular meshes. J. Sci. Comput. 15, 197–229.

Borges, R., Carmona, M., Costa, B., Don, W.S., 2008. An improved weighted essentially non-oscillatory scheme for hyperbolic conservation laws. J. Comput. Phys. 227, 3191–3211.

Casper, J., Shu, C.W., Atkins, H.L., 1994. Comparison of two formulations for high-order accurate essentially nonoscillatory schemes. AIAA J. 32, 1970–1977.

Castro, M., Costa, B., Don, W.S., 2011. High order weighted essentially non-oscillatory WENO-Z schemes for hyperbolic conservation laws. J. Comput. Phys. 230, 1766–1792.

Chou, C.S., Shu, C.W., 2006. High order residual distribution conservative finite difference WENO schemes for steady state problems on non-smooth meshes. J. Comput. Phys. 214, 698–724.

Ciarlet, P.G., Raviart, P.A., 1972. General Lagrange and Hermite interpolation in $\mathbf{R}^n$ with application to finite element methods. Arch. Ration. Mech. Anal. 42, 177–199.

Dumbser, M., Käser, M., 2007. Arbitrary high order non-oscillatory finite volume schemes on unstructured meshes for linear hyperbolic systems. J. Comput. Phys. 221, 693–723.

Dumbser, M., Käser, M., Titarev, V.A., Toro, E.F., 2007. Quadrature-free non-oscillatory finite volume schemes on unstructured meshes for nonlinear hyperbolic systems. J. Comput. Phys. 226, 204–243.

Friedrichs, O., 1998. Weighted essentially non-oscillatory schemes for the interpolation of mean values on unstructured grids. J. Comput. Phys. 144, 194–212.

Gottlieb, S., Shu, C.W., Tadmor, E., 2001. Strong stability-preserving high-order time discretization methods. SIAM Rev. 43, 89–112.

Gottlieb, S., Mullen, J.S., Ruuth, S.J., 2006. A fifth order flux implicit WENO method. J. Sci. Comput. 27, 271–287.

Grasso, F., Pirozzoli, S., 2001. Simulations and analysis of the coupling process of compressible vortex pairs: free evolution and shock induced coupling. Phys. Fluids 13, 1343–1366.

Hairer, E., Wanner, G., 1991. Solving Ordinary Differential Equations II, Stiff and Differential-Algebraic Problems. Springer, Berlin.

Hao, W., Hauenstein, J.D., Shu, C.W., Sommese, A.J., Xu, Z., Zhang, Y.T., 2013. A homotopy method based on WENO schemes for solving steady state problems of hyperbolic conservation laws. J. Comput. Phys. 250, 332–346.

Harten, A., Osher, S., Engquist, B., Chakravarthy, S., 1986. Some results on uniformly high order accurate essentially non-oscillatory schemes. Appl. Numer. Math. 2, 347–377.

Harten, A., Engquist, B., Osher, S., Chakravarthy, S., 1987. Uniformly high order essentially non-oscillatory schemes III. J. Comput. Phys. 71, 231–303.

Henrick, A.K., Aslam, T.D., Powers, J.M., 2005. Mapped weighted essentially non-oscillatory schemes: achieving optimal order near critical points. J. Comput. Phys. 207, 542–567.
Hu, C., Shu, C.W., 1999. Weighted essentially non-oscillatory schemes on triangular meshes. J. Comput. Phys. 150, 97–127.
Hu, G.H., Li, R., Tang, T., 2011. A robust WENO type finite volume solver for steady Euler equations on unstructured grids. Commun. Comput. Phys. 9, 627–648.
Hu, X.Y., Wang, B., Adams, N.A., 2015. An efficient low-dissipation hybrid weighted essentially non-oscillatory scheme. J. Comput. Phys. 301, 415–424.
Jiang, G., Shu, C.W., 1996. Efficient implementation of weighted ENO schemes. J. Comput. Phys. 126, 202–228.
Jiang, T., Zhang, Y.T., 2013. Krylov implicit integration factor WENO methods for semilinear and fully nonlinear advection-diffusion-reaction equations. J. Comput. Phys. 253, 368–388.
Jiang, T., Zhang, Y.T., 2016. Krylov single-step implicit integration factor WENO methods for advection-diffusion-reaction equations. J. Comput. Phys. 311, 22–44.
Kennedy, C.A., Carpenter, M.H., 2003. Additive Runge-Kutta schemes for convection-diffusion-reaction equations. Appl. Numer. Math. 44, 139–181.
Levy, D., Nayak, S., Shu, C.W., Zhang, Y.T., 2006. Central WENO schemes for Hamilton-Jacobi equations on triangular meshes. SIAM J. Sci. Comput. 28, 2229–2247.
Liu, Y., Zhang, Y.T., 2013. A robust reconstruction for unstructured WENO schemes. J. Sci. Comput. 54, 603–621.
Liu, X.D., Osher, S., Chan, T., 1994. Weighted essentially non-oscillatory schemes. J. Comput. Phys. 115, 200–212.
Martin, M.P., Taylor, E.M., Wu, M., Weirs, V.G., 2006. A bandwidth-optimized WENO scheme for the effective direct numerical simulation of compressible turbulence. J. Comput. Phys. 220, 270–289.
Ponziani, D., Pirozzoli, S., Grasso, F., 2003. Development of optimized weighted-ENO schemes for multiscale compressible flows. Int. J. Numer. Methods Fluids 42, 953–977.
Qiu, J., Shu, C.W., 2003. Finite difference WENO schemes with Lax-Wendroff-type time discretizations. SIAM J. Sci. Comput. 24, 2185–2198.
Qiu, J., Shu, C.W., 2005. Runge-Kutta discontinuous Galerkin method using WENO limiters. SIAM J. Sci. Comput. 26, 907–929.
Remacle, J.F., Flaherty, J.E., Shephard, M.S., 2003. An adaptive discontinuous Galerkin technique with an orthogonal basis applied to compressible flow problems. SIAM Rev. 45, 53–72.
Shi, J., Hu, C., Shu, C.W., 2002. A technique of treating negative weights in WENO schemes. J. Comput. Phys. 175, 108–127.
Shi, J., Zhang, Y.T., Shu, C.W., 2003. Resolution of high order WENO schemes for complicated flow structures. J. Comput. Phys. 186, 690–696.
Shu, C.W., Osher, S., 1988. Efficient implementation of essentially non-oscillatory shock capturing schemes. J. Comput. Phys. 77, 439–471.
Shu, C.W., Osher, S., 1989. Efficient implementation of essentially non-oscillatory shock capturing schemes II. J. Comput. Phys. 83, 32–78.
Shu, C.W., Zang, T.A., Erlebacher, G., Whitaker, D., Osher, S., 1992. High-order ENO schemes applied to two- and three-dimensional compressible flow. Appl. Numer. Math. 9, 45–71.
Taylor, E.M., Wu, M.W., Martin, M.P., 2007. Optimization of nonlinear error for weighted essentially non-oscillatory methods in direct numerical simulations of compressible turbulence. J. Comput. Phys. 223, 384–397.
Titarev, V.A., Toro, E.F., 2005. ADER schemes for three-dimensional non-linear hyperbolic systems. J. Comput. Phys. 204, 715–736.

Titarev, V.A., Tsoutsanis, P., Drikakis, D., 2010. WENO schemes for mixed-element unstructured meshes. Commun. Comput. Phys. 8, 585–609.

Toro, E.F., 2009. Riemann Solvers and Numerical Methods for Fluid Dynamics: A Practical Introduction. Springer-Verlag, Berlin, Heidelberg.

Wang, Z.J., Chen, R.F., 2001. Optimized weighted essentially nonoscillatory schemes for linear waves with discontinuity. J. Comput. Phys. 174, 381–404.

Wang, R., Spiteri, R.J., 2007. Linear instability of the fifth-order WENO method. SIAM J. Numer. Anal. 45, 1871–1901.

Wu, L., Zhang, Y.T., Zhang, S., Shu, C.W., 2016. High order fixed-point sweeping WENO methods for steady state of hyperbolic conservation laws and its convergence study. Commun. Comput. Phys. 20, 835–869.

Xiong, T., Zhang, M., Zhang, Y.T., Shu, C.W., 2010. Fast sweeping fifth order WENO scheme for static Hamilton-Jacobi equations with accurate boundary treatment. J. Sci. Comput. 45, 514–536.

Zhang, Y.T., Shu, C.W., 2003. High order WENO schemes for Hamilton-Jacobi equations on triangular meshes. SIAM J. Sci. Comput. 24, 1005–1030.

Zhang, S., Shu, C.W., 2007. A new smoothness indicator for the WENO schemes and its effect on the convergence to steady state solutions. J. Sci. Comput. 31, 273–305.

Zhang, Y.T., Shu, C.W., 2009. Third order WENO scheme on three dimensional tetrahedral meshes. Commun. Comput. Phys. 5, 836–848.

Zhang, Y.T., Shi, J., Shu, C.W., Zhou, Y., 2003. Numerical viscosity and resolution of high-order weighted essentially nonoscillatory schemes for compressible flows with high Reynolds numbers. Phys. Rev. E 68, 046709.

Zhang, S., Zhang, Y.T., Shu, C.W., 2005. Multistage interaction of a shock wave and a strong vortex. Phys. Fluids 17, 116101.

Zhang, S., Zhang, Y.T., Shu, C.W., 2006. Interaction of an oblique shock wave with a pair of parallel vortices: shock dynamics and mechanism of sound generation. Phys. Fluids 18, 126101.

Zhang, Y.T., Shu, C.W., Zhou, Y., 2006. Effects of shock waves on Rayleigh-Taylor instability. Phys. Plasmas 13, 062705.

Zhang, Y.T., Zhao, H.K., Chen, S., 2006. Fixed-point iterative sweeping methods for static Hamilton-Jacobi equations. Methods Appl. Anal. 13, 299–320.

Zhang, Y.T., Zhao, H.K., Qian, J., 2006. High order fast sweeping methods for static Hamilton-Jacobi equations. J. Sci. Comput. 29, 25–56.

Zhang, S., Jiang, S., Zhang, Y.T., Shu, C.W., 2009. The mechanism of sound generation in the interaction between a shock wave and two counter rotating vortices. Phys. Fluids 21, 076101.

Zhang, S., Jiang, S., Shu, C.W., 2011. Improvement of convergence to steady state solutions of Euler equations with the WENO schemes. J. Sci. Comput. 47, 216–238.

Zhu, J., Qiu, J., Shu, C.W., Dumbser, M., 2008. Runge-Kutta discontinuous Galerkin method using WENO limiters II: unstructured meshes. J. Comput. Phys. 227, 4330–4353.